

AMORPHOUS Cr-Ti LAYER FOR A HIGHLY (002) TEXTURED BCC Cr BASED ALLOY SEED LAYER FOR FePt-C HEAT-ASSISTED MAGNETIC RECORDING MEDIA

Akihiro SHIMIZU¹, Seong-Jae JEON², Shintaro HINATA³ and Shin SAITO⁴

- 1) Tohoku University, Sendai, Miyagi, 980-8579 JAPAN s.akihiro@ecei.tohoku.ac.jp
- 2) Tohoku University, Sendai, Miyagi, 980-8579 JAPAN, jsjgst@ecei.tohoku.ac.jp
- 3) Tohoku University, Sendai, Miyagi, 980-8579 JAPAN, s_hinata@ecei.tohoku.ac.jp
- 4) Tohoku University, Sendai, Miyagi, 980-8579 JAPAN, ssaito@ecei.tohoku.ac.jp

I. INTRODUCTION

Heat-assisted magnetic recording (HAMR) media based on L1₀ FePt granular film is considered to extend the maximum areal density over 4 Tb/in² owing to the high magnetocrystalline anisotropy of L1₀ ordered phase for FePt ($K_u \sim 7 \times 10^7$ erg/cm³) [1–3]. In order to realize the L1₀ ordered FePt granular film as a high recording density medium, it is necessary to enhance signal-to-noise ratio (SNR). Contribution to the SNR can result from variation in the angular distribution of *c*-axis orientation of L1₀ grains. Since the *c*-axis orientation, which corresponds to the easy magnetized axis for the L1₀ ordered FePt, can be adjusted by hetero-epitaxial growth from (002) textured crystalline seed layer (SL), the angular distribution of the *c*-axis is mainly attributed to that of SL. Recently, we reported the concept to suppress the angular distribution of the (002) orientation of SL [4]. The origin of the angular distribution of the crystal orientation can be described by considering the formation of crystalline facets during the solidification of liquid phase of sputtered atoms under the different wettability of SL on an amorphous-texture inducing layer (*a*-TIL). Low wettability condition induces the ball-shaped liquid phase of the sputtered atoms, whereas high wettability condition tends to spread the liquid phase over surface of *a*-TIL. During the solidification, the liquid phase changes to the crystalline facet in order to form the crystallographic texture. In the case of the low wettability, the crystalline facets have much more chance to form the crystalline plane with various angles from normal to the film plane. Consequently, the crystallographic texture can be slanted from normal to the film plane. In the case of the high wettability, the most surface of the crystalline facets is parallel to the normal to the plane, which induces the development of the crystallographic texture without a tilt of the crystal orientation. Providing that the texture is determined by the solidification, fabrication of the large grain SL is important. Based on the concept, a designed stacking structure is illustrated in Fig. 1. We found that the materials combination between bcc-Cr alloy SL and Cr₅₀Ti₅₀ *a*-TIL promoted the lateral grain growth for bcc-Cr alloy SL. However, crystallization of the Cr₅₀Ti₅₀ *a*-TIL suppressed the development of the lateral grain growth. In order to increase the grain size of bcc-Cr alloy SL, investigation on the degree of amorphous and thermal stability of amorphous is inevitable. In this research, quantitative study on the amorphous Cr-Ti TILs was carried out for (002) texture formation of bcc-Cr alloy SL.

II. RESULTS AND DISCUSSION

Figure 2 shows in-plane XRD patterns of (a) as-deposited and (b) post-annealed up to a temperature of 600 °C for Cr_{100-x}Ti_x(20 nm) TILs on NiTa(2 nm)/glass substrate with various Ti content. In the case of (a) as-deposited state, two diffractions at Bragg angles of $2\theta_\chi = 44^\circ$ and 64° were observed in $x = 0$ (pure bcc-Cr) TIL. These diffractions, which are identified as (110) and (220) diffractions of bcc-Cr powder, gradually shifted to lower angles with the increase of $x = 0$ to 20 at%. The result indicates that the atomic substitution from Cr to Ti induces the increase of the lattice volume while sustaining the crystalline structure. However, change of the diffraction width from the narrow to broad signal was observed with the further increase of x from 20 to 30 at%, and then the broad signal was confirmed regardless of the increase of x up to 75 at%. This result suggests that the amount of the constructive interference of X-rays decreases due to the randomly located atoms (i.e. amorphous phase). Again, two diffractions at Bragg angles of $2\theta_\chi = 35^\circ$ and 63° were obtained in $x = 100$ (pure hcp-Ti) TIL. In the case of (b) post-annealed TILs, one can see that additional diffractions exist at $2\theta_\chi = 40 \sim 44^\circ$ and 64° in $x = 30, 70,$ and 75 at% as compared

Akihiro SHIMIZU

tel: +81-296-25-3438

s.akihiro@ecei.tohoku.ac.jp

with the as-deposited TILs. The result suggests that these films are crystallized. Only the films with x from 40 to 60 at% maintained the amorphous phase against the heat treatment.

Figure 3 shows the angular distribution of (002) crystal orientation of bcc-SL derived from full width at half maximum (FWHM) plotted against T_{sub} and x . Measured range for (002) sheet texture (gray region) is limited by both $T_{\text{sub}} \geq 300^\circ\text{C}$ and $30 < x$ (at%) < 75 . Note that this composition range corresponds to the amorphous formation region for $\text{Cr}_{100-x}\text{Ti}_x$ TILs. In addition, magnitude of FWHM along the same x decreased with increasing T_{sub} (solid circle ●) and then, decreased with further increasing T_{sub} (open circle ○) within x of 50 to 70 at%.

At the presentation, relation between Ti content and grain diameter of the CrMn seed layer, and magnetic properties of FePt-C will be discussed.

REFERENCES

- 1) M. H. Kryder, E. C. Gage, T. W. McDaniel, W. A. Challener, R. E. Rottmayer, G. Ju, Y.-T. Hsia, and M. F. Erden, *Proc. IEEE*, **96**, 1810 (2008).
- 2) A. Q. Wu, Y. Kubota, T. Klemmer, T. Rausch, C. Peng, Y. Peng, D. Karns, X. Zhu, Y. Ding, E. K. C. Chang, Y. Zhao, H. Zhou, K. Gao, J.-U. Thiele, M. Seigler, G. Ju, and E. Gage, *IEEE Trans. Magn.*, **49**, 779 (2013).
- 3) X. Wang, K. Gao, H. Zhou, A. Itagi, M. Seigler, and E. Gage, *IEEE Trans. Magn.*, **49**, 686 (2013).
- 4) Seong-Jae Jeon, Shintaro Hinata, Shin Saito, and Migaku Takahashi, *J. Appl. Phys.*, **117**, 17A924 (2015).

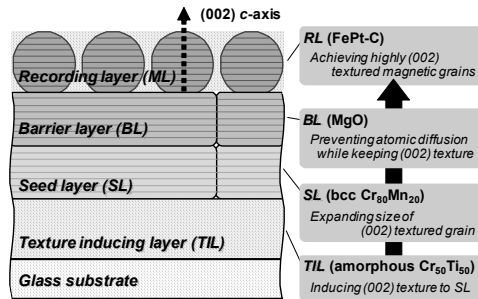


Fig. 1 Schematic representation to suppress angular distribution of (002) c -axis orientation for FePt-C granular film

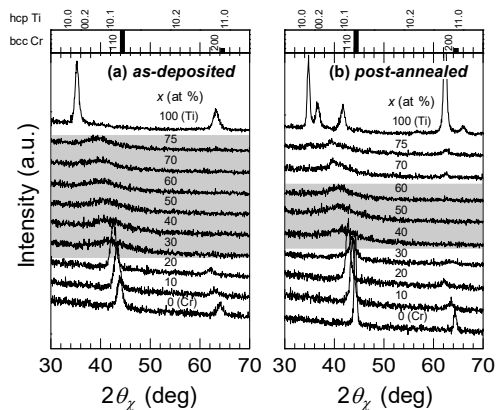


Fig. 2 In-plane XRD patterns of (a) as-deposited and (b) post-annealed $\text{Cr}_{100-x}\text{Ti}_x$ (20 nm) TILs on NiTa (2 nm)/glass substrate with various Ti compositions, x .

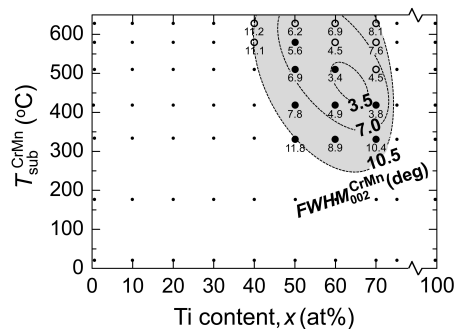


Fig. 3 Angular distribution of CrMn (002) crystal orientation (FWHM) varied with substrate temperature (T_{sub}) and Ti composition, x .